Reflection Full Waveform Inversion for a Wide-azimuth Dataset in the Gulf of Mexico

Z. Zou* (PGS), J. Ramos-Martínez (PGS), A.A. Valenciano (PGS) & S. Kelly (PGS)

SUMMARY

Full waveform inversion (FWI) iteratively minimizes the misfit between the recorded and modelled seismic data to derive an accurate velocity model. The method can produce high-resolution velocity models, provided that the target areas are well-sampled by the seismic waves (e.g. shallow targets with refracted waves and deep targets with reflected waves). Here, we present an application of FWI to a wide-azimuth dataset from the Gulf of Mexico. Due to the large water depth, refracted and diving waves are not well represented in the recorded data. Thus, the inversion must rely on the reflected waves. This in turn places more stringent requirements on the fidelity of the computed amplitudes, so variable density was included in the inversion. Through reflection FWI, we were able to obtain a velocity model with much higher resolution than is shown in the preliminary, ray-tomography model. We observed that the FWI model improve the flatness of common-image gathers and the quality of the stacked, migrated images. Furthermore, the small-scale velocity features revealed by FWI correlated well with the migrated image.

Introduction

The goal of full-waveform inversion (FWI) is to derive high-resolution Earth models by minimizing the misfit between the recorded and model data to achieve high-resolution imaging and provide insights into reservoir characterization. This is a highly nonlinear, iterative process whose success depends on the seamless addition of wavelength features that are missing from the starting velocity model. The appropriate method for the introduction of these missing wavelengths depends on the characteristics of the geological setting and the seismic wave types that were acquired. In shallow water, the recorded refracted and diving waves provide an optimal opportunity for FWI to resolve the small-scale, shallow structures, at depths up to the deepest turning point (e.g. Sirgue et al., 2009; Warner et al., 2013; Zou et al., 2014). In contrast, there have been far fewer successful applications of FWI to streamer seismic data in deep water. The reason for this is that refracted and diving waves are often not recorded, due to the limited streamer length. FWI must thus rely on the low-frequency content of the reflected waves to enable a continuous velocity update for the range of spatial wavenumbers that are missing from the starting model (e.g. Vigh et al., 2010; Ramos-Martinez et al., 2013). An improved velocity model derived from reflection FWI can potentially lead to better salt interpretation and superior subsalt imaging.

Here, we applied reflection FWI to a wide-azimuth dataset acquired in deep water in the Gulf of Mexico (GOM), with a maximum in-line offset of 7 km and a maximum cross-line offset of 4.2 km. Our initial inversion results showed an improved image in the sediments above the salt.

Data and method

The data were acquired for a wide-azimuth, towed-streamer, shooting geometry that consisted of two recording vessels. Each vessel was equipped with a single source and 10 streamers. Between the recording vessels, there were two additional source vessels. The effective spacing between sail lines was 600 meters. The streamer separation was 120 m and the cable length was 7000m. This yielded a maximum offset in the cross-line direction of 4200 m. The source depth was 9 m and the receiver depth was 12 m. The water depth for the FWI test area varied from 1200 m to 1500 m.

Our time-domain inversion used the method of conjugate gradients, with each gradient computed by the adjoint-state method. The forward modelling was performed using a pseudo-analytic (PA), anisotropic extrapolator. Details and advantages for extrapolation by the PA method are reviewed in Ramos-Martinez et al. (2011). The inversion of reflections requires a more accurate modelling of the amplitudes than inversion by refractions and diving waves, so variable density was considered in the modelling engine. In order to minimize the likelihood of cycle skipping, the inversion started with the lowest possible frequency that exhibited coherent signal in the recorded data. In this case, we applied a Butterworth, low-pass filter of 5Hz, with a slope of 50dB/octave, to the input data. After a series of QC steps, we then increased the maximum frequency to 7Hz in order to further enhance the resolution of the velocity model.

The starting velocity and anisotropy models for FWI were obtained from travel time tomography and well logs, and the density model was derived based on Gardner's equations (Gardner et al., 1974). The water density was set to 1.027 g/cm, and salt density was set to 2.17g/cm. During the inversion, only the velocity was updated, while the density and anisotropy models were held fixed.

Inversion results

Figures 1(a) and 1(b) show an inline section of the tomography and FWI velocity models, respectively. Figures 1(c) and 1(d) compare the two models in a cross-line section. In general, the model derived by FWI has much higher resolution than the smooth, tomography model. In order to evaluate the model derived by FWI, we performed Kirchhoff, pre-stack depth migration. We observed that the FWI velocity model improved the flatness of common-image gathers, as shown in figures 2(a) and 2(b).

Figures 3(a) and 3(b) compare a vertical section of migrated stacks for the tomography and FWI models, respectively. The horizons in figure 3(a) clearly have better signal-to-noise ratio and continuity, as indicated in the circled areas. Figures 3(c) and 3(d) compare the migrated stacks for another vertical section, for the two velocity models. The stack generated using the FWI velocity shows clearer delineation of the faults.

In order to further validate the FWI velocity models, we compare velocity depth slices to the migrated image. Figures 4 and 5 display these comparisons at depths of 1700m and 3500m, respectively. Many small-scale velocity features are observable in the FWI model, but not in the tomography model, and they correlate very well with geological features in the migrated image. For instance, figure 4(b) shows three distinctive, low-velocity patches that are very consistent with the features in the image, as highlighted by three red ellipses in figure 4(d). The lineations in figure 5(b) are also consistent with the corresponding image.

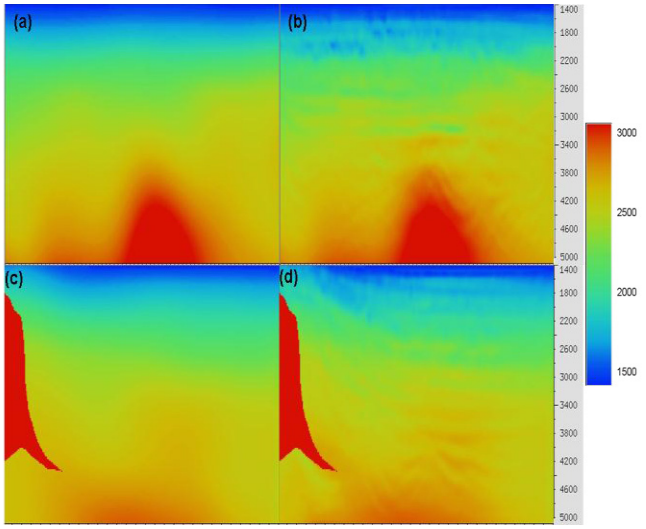

Figure 1 *In-line sections of (a) tomography velocity and (b) FWI velocity, and across-line sections of (c) tomography velocity and (d) FWI velocity.*

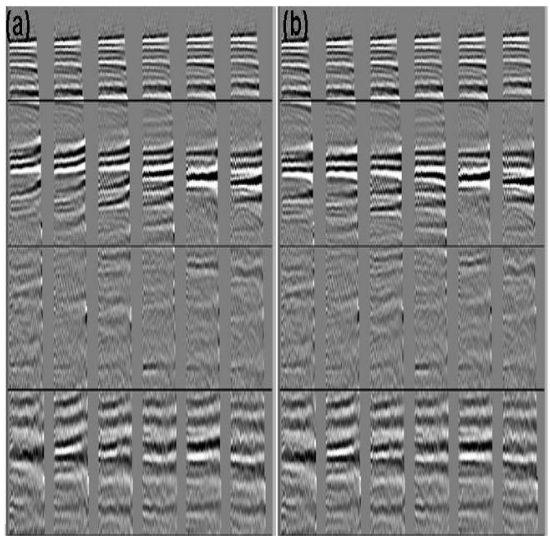

Figure 2 *Common-image, offset gathers computed using (a) tomography model and (b) FWI model.*

Conclusions

We applied reflection FWI to a wide-azimuth dataset acquired in deep water in the GOM. FWI produced a velocity model with much higher resolution compared to the velocity model from conventional tomography. The small-scale velocity features revealed by FWI correlated very well with the geological features in the migrated image. We also observed that the FWI model improved the flatness of common-image gathers and the quality of the migrated images overall. Migration using the FWI model yields more continuous reflectors, better focused and defined faults, and an overall improvement in the signal-to-noise ratio of the image.

Acknowledgement

The authors would like to thank Steve Smith and Jack Kinkead for the pre-processing work. We also thank Nizar Chemingui, Sverre Brandsberg-Dahl, Sean Crawley and John Cramer for discussions and suggestions. We thank PGS management for the opportunity to publish this work.

Reference

Gardner, G.H.F., Gardner, L.W., and Gregory, A.R. [1974] Formation velocity and density – the diagnostic basics for stratigraphic traps, Geophysics, 39, 770-780.

Ramos-Martinez, J., Crawley, S., Kelly, S., and Tsimelzon, B. [2011] Full-waveform inversion by pseudo-analytic extrapolation, 81st Annual Meeting, SEG, Expanded Abstracts, 2684–2688.

Ramos-Martinez, J, Zou, K., Kelly, S., Tsimelzon, B. [2013] Reflection FWI from fully deghosted towed-streamer data: A field data example. 83rd Annual International Meeting, SEG, Expanded Abstracts 2013: 887-891.

Sirgue, L., Barkved, O.J., Van Gestel, J.P, Askim, O.J. and Kommedal, J.H. [2009] 3D waveform inversion on Valhall wide-azimuth OBC, 71st EAGE Conference & Exhibition, Extended Abstracts, U038.

Vigh, A. Starr, B., Kapoor, J., and Li, H. [2010] 3D Full Waveform Inversion on a Gulf of Mexico WAZ Data Set, 80th Annual Meeting, SEG, Expanded Abstracts, 957-961.

Warner, M., Ratcliffe, A., Nangoo, T., Morgan, J., Umpleby, A., Shah, M., Vinje, V., Štek, I., Guasch, L., Win, C., Conroy, G. and Bertrand, A. [2013] Anisotropic 3D full-waveform inversion, Geophysics, 78, R59-R80.

Zou, Z., Ramos-Martínez, J., Kelly, S., Ronholt, G., Langlo, L.T., Valenciano Mavilio, A., Chemingui, N. and Lie, J.E. [2014] Refraction Full-waveform Inversion in a Shallow Water Environment, 76th EAGE Conference & Exhibition, Extended Abstracts, E106

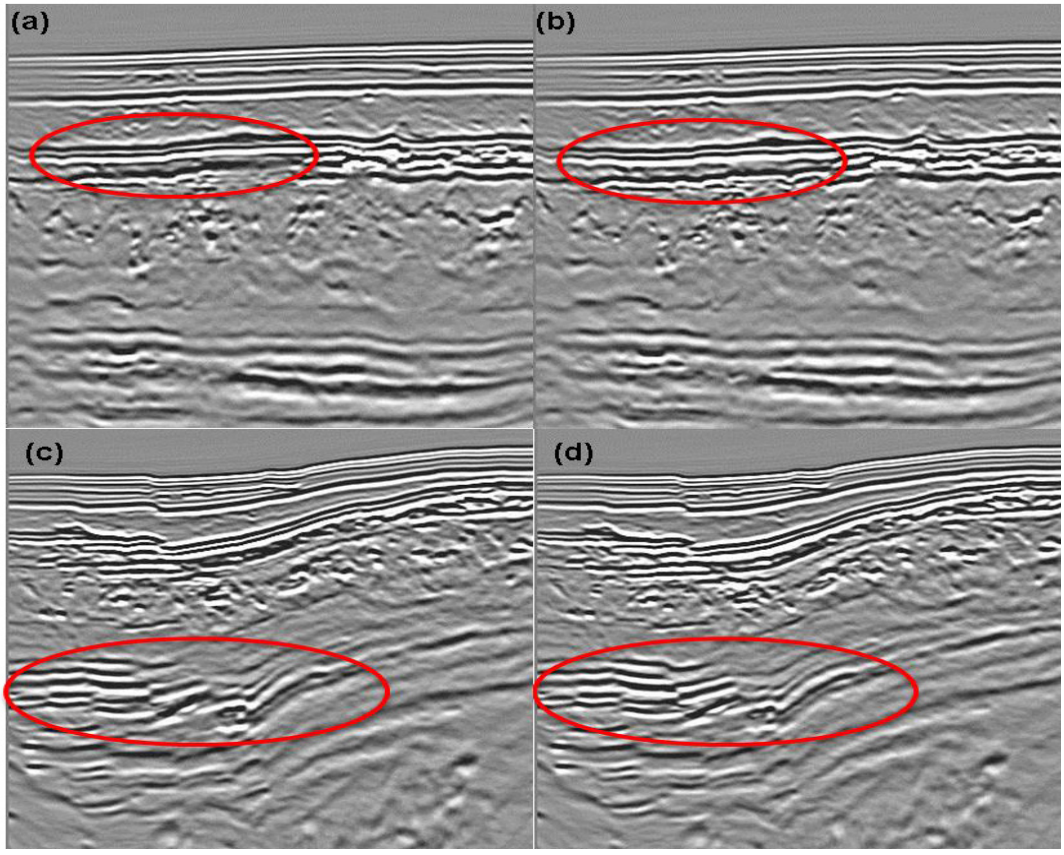

Figure 3 *(a) and (b) are vertical slices of migrated images obtained using tomography and FWI models, respectively. (c) and (d) provide the same comparison for another vertical slice.*

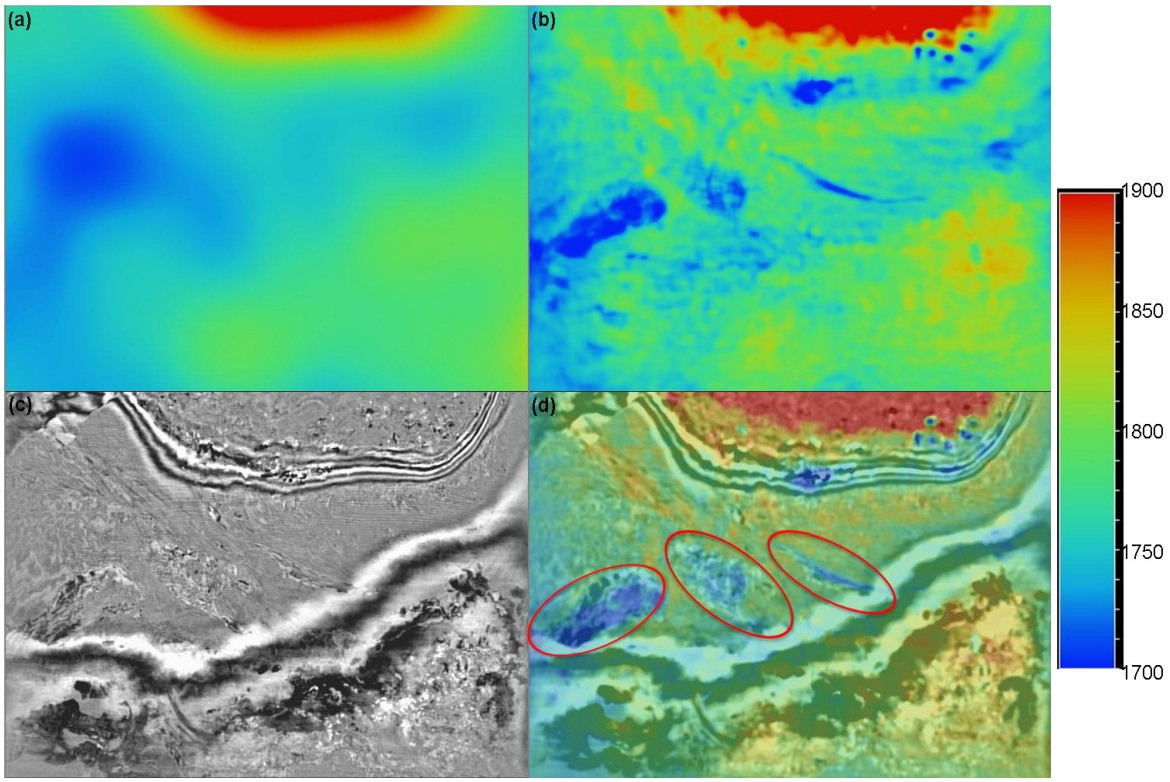

Figure 4 *Depth slices at 1700m for (a) tomography velocity, (b) FWI velocity, (c) Kirchhoff migrated image with FWI velocity and (d) overlay of FWI velocity and the image.*

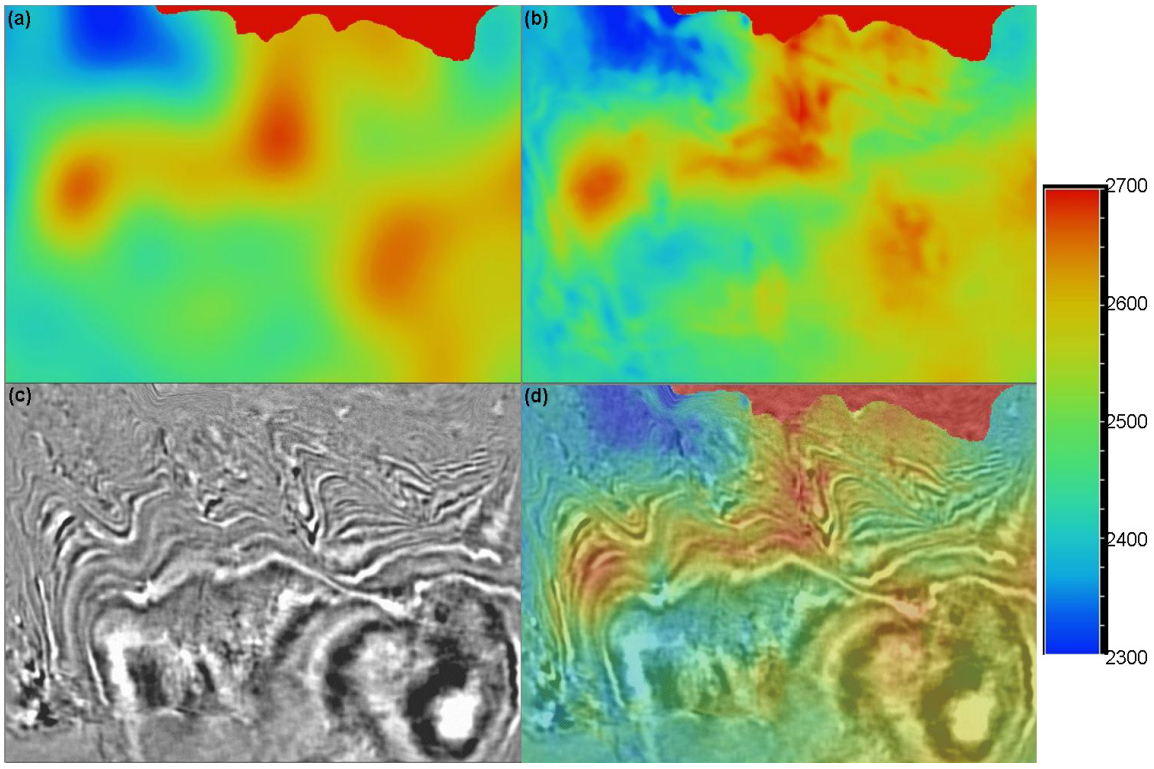

Figure 5 *Depth slices at 3700m for (a) tomography velocity, (b) FWI velocity, (c) Kirchhoff migrated image with FWI velocity and (d) overlay of FWI velocity and the image.*